

Article

Design a Stratiform Metamaterial with Precise Optical Property

Yi-Jun Jen *  and Wei-Chin Liu

Department of Electro-Optical Engineering, National Taipei University of Technology, No. 1, Sec. 3, Chung-Hsiao E. Rd. Taipei, Taiwan; lineage107@yahoo.com.tw

* Correspondence: jyjun@ntut.edu.tw

Received: 19 October 2019; Accepted: 28 November 2019; Published: 1 December 2019



Abstract: In this work, a stratiform metamaterial is arranged as multiple periods of metal-dielectric symmetrical film stack to provide precise equivalent refractive index and admittance. There are multiple solutions of equivalent refractive index retrieved from the characteristic matrix of the film stack. The correct refractive index is derived by connecting different branches of solution at different ranges of wavelength or thickness of the dielectric layer. The refractive index of an Ag-TiO₂ five-layered symmetrical film stack shown in previous work is demonstrated to be positive real instead of negative real. The associated type I iso-frequency curve supports negative refraction. In order to extend the operating wavelength of type I metamaterial, the number of the metal-dielectric symmetrical film stack is increased to reduce the thickness of the dielectric film to approach subwavelength requirement.

Keywords: metamaterial; symmetrical film stack; negative refraction

1. Introduction

A metamaterial with a negative index of refraction has been predicted to be effective for constructing a perfect lens [1]. Archetypical left-handed metamaterials comprise split rings as inductive-capacitive resonators, which support the simultaneous reversal of electric and magnetic responses to light at microwave frequencies [2]. Using advanced lithographic nanofabrication, the scales of resonators were shrunk to exhibit a left-handed response to light at higher frequencies, such as infrared or visible frequencies [3]. Recently, a stratiform metamaterial that comprises metal film (M) and dielectric film (D) was developed for transverse magnetic (TM) polarization mode [4]. Light incident on the side of this stack will couple to waveguide modes [5,6]. The anti-symmetry mode of the transverse electric field in a plasmonic waveguide composed of metal film (M)/dielectric film (D)/metal film (M) (MDM) causes a negative group velocity at frequencies greater than the surface plasmon resonance frequency [6]. A combination of a pair of typical MDM waveguides as a waveguide composed of metal film (M)/dielectric film (D)/metal film (M)/dielectric film (D)/metal film (M) (MDMDM) results in electric-field coupling between adjacent MDM waveguides. The symmetrical electric field distribution leads to a positive coupling constant, thus the stack exhibits backward wave phenomenon.

In 2014, a film stack comprising TiO₂ and Ag films alternately was claimed to yield an index of negative unity over a wide range of incidence angles at a wavelength of 363.8 nm [7]. Later, whether the negative refraction in the TiO₂-Ag multilayer came from a negative index of refraction was questioned and discussed. The negative refraction also occurs in a hyperbolic metamaterial. Hyperbolic metamaterials have been developed for more than 10 years. In most cases, hyperbolic metamaterials are metal-dielectric multilayers [8,9]. Its property is described by a diagonal permittivity tensor. The principal permittivities are roughly estimated using effective medium approximation [10]. The signs of the two tangential permittivities are the same, but the signs of its tangential and vertical permittivities are opposite. Accordingly, there are two kinds of hyperbolic shaped isofrequency curves

(type I and type II) [11]. A previous work on the decomposition of the Bloch wave in the layered structure into a number of harmonics showed that the iso-frequency curve of the main harmonic mode corresponds to the type I hyperbolic metamaterial [12]. The negative refraction of energy is invoked by the shape of the iso-frequency contour [11]. Therefore, the multilayer is a hyperbolic metamaterial, and light propagation is mainly dominated by right-handed harmonics with a positive phase index.

Although the relevant works have explained the wave phenomenon in a metal-dielectric multilayer, a comprehensive design method for negative refraction is still required. A multilayer with precise optical constants, including refractive index and admittance, are necessary for a metamaterial design because, in real applications, both transmission and reflection are affected by both optical constants. In this work, a stratiform metamaterial is designed by arranging a multilayer composed of multiple periods of metal-dielectric symmetrical film stack (SFS). Based on the calculation of characteristic film matrixes [13], the metal-dielectric symmetrical film stack is equivalent to a layer with the equivalent refractive index and admittance that can be derived precisely by choosing the correct solution from a multi-branch of solution [14,15]. The refractive index versus angle of incidence can be used to plot a precise iso-frequency curve that indicates whether the stratiform metamaterial is a hyperbolic metamaterial. A type I hyperbolic metamaterial supports negative refraction from normal incidence to a certain oblique angle of incidence. In order to apply to real applications, the transmission is taken into account by considering the extinction coefficient and admittance [16].

2. Methods

Exploiting thin-film optics, symmetrical film stacks have been widely designed for edge filters [17]. An all-dielectric symmetrical film stack is equivalent to a single layer with an equivalent refractive index that is a function of wavelength λ , thicknesses, and refractive indexes of all constituent films. The equivalent refractive index is pure real and pure imaginary in different wavelength ranges, providing passband and stopband characteristics, respectively. An edge filter was designed across the passband and stopband. The equivalent model of a metal-dielectric symmetrical film stack was still valid, thus the product of characteristic film matrixes of the constituent thin films yielded a resultant matrix that had the same form of that of a single layer. Figure 1 shows the equivalent model of 3 symmetrical films composed of film A and film B. Equation (1) shows the product of 3 characteristic film matrixes of the symmetrical structure: film A/film B/film A (ABA).

$$\begin{aligned} \begin{bmatrix} M_{11} & M_{12} \\ M_{21} & M_{22} \end{bmatrix} &= \begin{bmatrix} \cos \delta_A & \frac{i}{\eta_A} \sin \delta_A \\ i\eta_A \sin \delta_A & \cos \delta_A \end{bmatrix} \begin{bmatrix} \cos \delta_N & \frac{i}{\eta_N} \sin \delta_N \\ i\eta_N \sin \delta_N & \cos \delta_N \end{bmatrix} \begin{bmatrix} \cos \delta_A & \frac{i}{\eta_A} \sin \delta_A \\ i\eta_A \sin \delta_A & \cos \delta_A \end{bmatrix} \\ &= \begin{bmatrix} \cos \gamma_{eq} & \frac{i}{E_{eq}} \sin \gamma_{eq} \\ iE_{eq} \sin \gamma_{eq} & \cos \gamma_{eq} \end{bmatrix} \end{aligned} \quad (1)$$

where δ_j and η_j ($j = A, B$) are the phase and admittance of each layer of the stack. The equivalent phase thickness of the stack γ_{eq} and the equivalent admittance E_{eq} were complex. At normal incidence, the equivalent refractive index N_{eq} is derived from the phase thickness γ_{eq} through the relationship $\gamma_{eq} = 2\pi N_{eq}(2d_A + d_B)/\lambda$. Both E_{eq} and N_{eq} can be tailored separately. Both E_{eq} and N_{eq} are represented with the equivalent permittivity ϵ_{eq} and the equivalent permeability μ_{eq} as $E_{eq} = \sqrt{\epsilon_{eq}/\mu_{eq}}$ and $N_{eq} = \sqrt{\epsilon_{eq}\mu_{eq}}$, respectively. According to effective medium approximation, the equivalent refractive index and admittance of a metal-dielectric composite are generally complex. In case of oblique incidence and TM polarization state, the equivalent phase thickness should be $\gamma_{eq}^{TM} = 2\pi N_{eq}(2d_A + d_B) \cos \theta_{eq}/\lambda$. Figure 1 shows the equivalent scheme of a 3-layered symmetrical film stack ABA. The θ_{eq} is the equivalent angle of refraction in the film stack. The d_A and d_B are thicknesses of film A and film B, respectively. The θ_A and θ_B are angles of refraction in film A and film B, respectively. The

equivalent admittance for TM polarization should be modified as $E_{eq}^{TM} = E_{eq} / \cos \theta_{eq}$. The product of the 3 characteristic film matrixes ABA is shown in Equation (2).

$$\begin{bmatrix} M_{11} & M_{12} \\ M_{21} & M_{21} \end{bmatrix} = \begin{bmatrix} \cos \gamma_{eq}^{TM} & \frac{i}{E_{eq}^{TM}} \sin \gamma_{eq}^{TM} \\ iE_{eq}^{TM} \sin \gamma_{eq}^{TM} & \cos \gamma_{eq}^{TM} \end{bmatrix} \quad (2)$$

The permittivity ε_{eq} can be retrieved from the matrix elements firstly through Equation (3).

$$\varepsilon_{eq} = E_{eq} N_{eq} = \frac{\lambda}{2\pi(2d_A + d_B)} \cos^{-1}(M_{11}) \sqrt{\frac{M_{21}}{M_{12}}} \quad (3)$$

The equivalent angle of refraction can be derived through the law of refraction $N_0 \sin \theta_0 = N_{eq} \sin \theta_{eq}$ (N_0 and θ_0 are the refractive indexes of the cover medium and angle of incidence, respectively), as shown in Equation (4).

$$\theta_{eq} = \tan^{-1} \left(\frac{N_{eq} \sin \theta_{eq}}{N_{eq} \cos \theta_{eq}} \right) = \tan^{-1} \left(\frac{N_0 \sin \theta_0}{\gamma_{eq} \left(\frac{\lambda}{2\pi(2d_A + d_B)} \right)} \right) = \tan^{-1} \left(\frac{N_0 \sin \theta_0}{\cos^{-1}(M_{11}) \left(\frac{\lambda}{2\pi(2d_A + d_B)} \right)} \right) \quad (4)$$

Next, we can get the equivalent refractive index N_{eq} shown in Equation (5).

$$N_{eq} = \sqrt{(N_{eq} \cos \theta_{eq})^2 + (N_{eq} \sin \theta_{eq})^2} = \sqrt{\left(\cos^{-1}(M_{11}) \left(\frac{\lambda}{2\pi(2d_A + d_B)} \right) \right)^2 + (N_0 \sin \theta_0)^2} \quad (5)$$

Finally, we can have the equivalent permeability μ_{eq} and admittance E_{eq} .

$$\mu_{eq} = (N_{eq})^2 \frac{1}{\varepsilon_{eq}} \quad (6)$$

$$E_{eq} = \sqrt{\varepsilon_{eq} / \mu_{eq}} \quad (7)$$

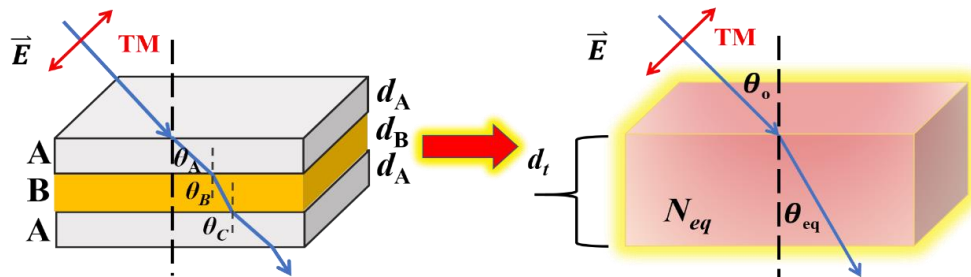


Figure 1. The equivalent model of a three-layered symmetrical film stack.

In this work, the time-dependent phase factor of a propagating harmonic wave takes the form $e^{i\omega t}$ (ω is the angular frequency) and an absorbing material has a refractive index $n-ik$. Unlike an all-dielectric symmetrical film stack, most metal–dielectric symmetrical film stacks have a different equivalent refractive index and equivalent admittance because the equivalent permeability μ_{eq} is not unity for most metal–dielectric composites in subwavelength scale. Both N_{eq} and E_{eq} can be tailored separately for novel applications [16]. In a previous work, a 7-layered metal–dielectric symmetrical film stack was designed and fabricated to have an E_{eq} near unity and an N_{eq} with large imaginary part that was comparable to that of a metal. Such a layered metamaterial can couple most incident light into the upper interface and dissipate its energy with a very small thickness [18].

It is noted that there were multi-solutions for the phase thickness and refractive index. There were multiple branches of solutions of equivalent phase thickness retrieved from matrix element M_{11} :

$\gamma_{eq} = \cos^{-1}(M_{11}) + m2\pi$ ($m = 0, \pm 1, \pm 2, \dots$). The correct solution should satisfy the 3 criteria: (1) The real part of the equivalent admittance should be positive; (2) the imaginary part of the equivalent refractive index should be negative; (3) both $N_{eq} = n_{eq} - ik_{eq}$ and $E_{eq} = E_r + iE_i$ as functions of wavelength or any constitutive parameter should be continuous [19]. It is particular that a specific branch was unable to satisfy the criteria over the whole wavelengths. The continuity of the real part of the equivalent refractive index as a function of wavelength or any constitutive parameter required choosing different branches for regions separated by the discontinuous points. For a metal-dielectric SFS in the form of MDM ... DM, a m -th branch was chosen thus that the n_{eq} at thickness of dielectric layer $d = 0$ was equal to the refractive index of metal. The m -th branch was correct for the range from $d = 0$ to its first discontinuous point at $d = d_{c1}$. The n_{eq} at thickness d larger than d_{c1} relied on a branch next to the m -th branch to connect the m -th branch at $d = d_{c1}$ to keep the continuous condition till its discontinuous point at $d = d_{c2}$. The correct branch for the thickness d larger than d_{c2} was chosen to keep continuous at the $d = d_{c2}$.

3. Results

A five-layered SFS of Ag (33 nm)/TiO₂ (28 nm)/Ag (30 nm)/TiO₂ (28 nm)/Ag (33 nm) in a previous work [7] was examined here. Such SFS was claimed to have a negative index around -1 at a wavelength of 363.8 nm. The refractive indexes of Ag and TiO₂ were 0.0785-1.59i and 2.8-0.05i, respectively. The equivalent n_{eq} versus thickness of TiO₂ from 0 nm to 60 nm at normal incidence with branch ($m = 0$) is shown in Figure 2a. At the thickness of $d = 0$ nm, the index of refraction was 0.0785, which was the real part of the refractive index of Ag. It means that the branch $m = 0$ was correct from $d = 0$ nm to its first discontinuous point at $d_{c1} = 22$ nm. At the thickness of $d = 28$ nm in Figure 2a, the index of refraction was -1.058, which was the proposed value of negative index. However, the index of refraction after $d_{c1} = 22$ nm needed to be connected with another branch ($m = 1$), as shown in Figure 2b. For the branch ($m = 1$), there was a discontinuous point at $d_{c2} = 37$ nm, thus the index after $d = 37$ nm was connected with branch ($m = -1$), as shown in Figure 2c. Figure 2d shows the correct real part of N_{eq} as a function of d from $d = 0$ nm to $d = 60$ nm.

Figure 3a shows both the real part and imaginary part of N_{eq} as a function of d . The n_{eq} at $d = 28$ nm was 1.34 and the N_{eq} versus the angle of incidence is shown in Figure 3b. With the correct N_{eq} as a function of angle of incidence. The iso-frequency curve (IFC) in Figure 3c represents the wave vector component k_z versus the other component k_x . The wave vector component along the interface is denoted as k_x that is decided by the incident wave vector k_0 and continuous across each interface of a multilayer. The other wave vector component perpendicular to the interface is k_z that can be derived through dispersion relation, as shown in Equation (8).

$$k_z = \pm \sqrt{\left(\frac{2\pi}{\lambda} N_{eq}\right)^2 - k_x^2} \quad (8)$$

The IFC shows that the multilayer is a type I hyperbolic metamaterial. Compared with the IFC estimated by effective permittivity tensor, the IFC calculated using the SFS equivalent model is precise. The ray vector derived from the IFC demonstrates that the imaging using the multilayer as a flat lens was based on the negative refraction instead of the nature of the negative index of refraction.

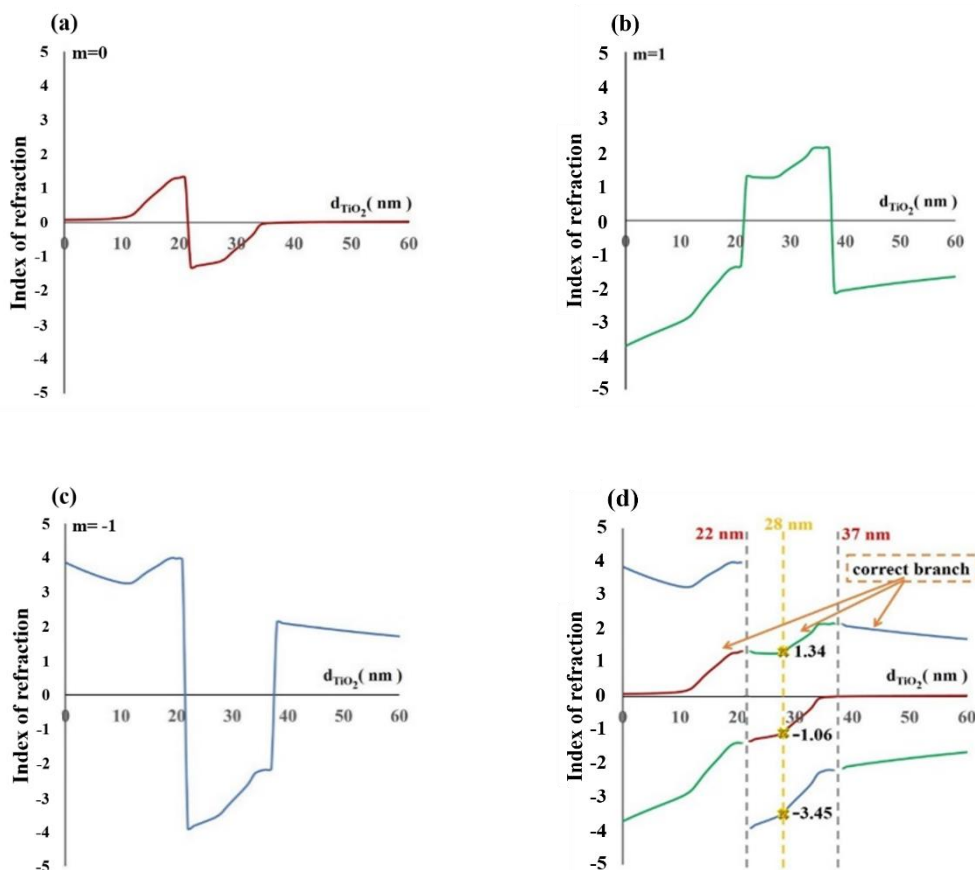


Figure 2. Equivalent n_{eq} of branches (a) $m = 0$, (b) $m = 1$, and (c) $m = -1$; (d) The correct n_{eq} as a function of d .

Here an SFS arrangement was used to design a type I hyperbolic metamaterial in order to provide a precise iso-frequency curve. High transmission at normal incidence was necessary for a type I metamaterial. The thicknesses of the metal and dielectric films needed to be within the subwavelength scale. However, the type I iso-frequency curve of an alternatively arranged metal–dielectric multilayer usually occurs at short wavelengths around the plasmonic resonance wavelength of the metal at which the permittivity of the metal film lead to low loss [20,21]. Besides the requirement of refractive index for type I isofrequency curve, the admittance should match to environment (air in this work) from normal incidence to an oblique angle to support the function of imaging. In order to overcome the frequency restriction for the occurrence of negative refraction, the type I hyperbolic metamaterial composed of Ag and Ta₂O₅ films was designed at a wavelength of 600 nm. According to our previous work [22], a thin metal film can be inserted between two metal films to perform a huge admittance locus and admittance matching to achieve high transmission property. The method, called modified Fabry-Perot (FP) design, can be extended to any odd-numbered metal–dielectric film stack. At a wavelength of 600 nm, the silver film usually takes 10 nm to 20 nm to achieve the modified FP design. Therefore, each silver film in the film stack was set to have the same thickness of 20 nm for the five-layered symmetrical film stack MDMDM = Ag/Ta₂O₅/Ag/Ta₂O₅/Ag. The optical constants of Ag and Ta₂O₅ were adopted from the commercial optical thin-film software (Essential Macleod) [23].

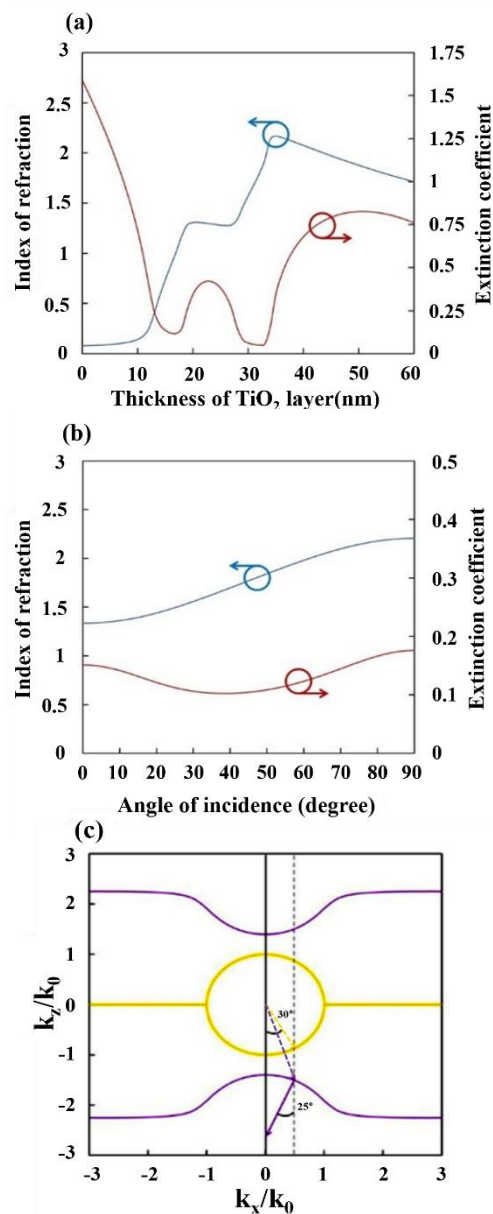


Figure 3. (a) Correct n_{eq} and k_{eq} as functions of d , (b) correct n_{eq} and k_{eq} as functions of angle of incidence at $d = 28$ nm, (c) the iso-frequency curve, the yellow and purple lines are cover medium and hyperbolic metamaterial, respectively. The dotted arrows and solid arrows represent wave vector and ray vector, respectively.

Figure 4a shows n_{eq} and k_{eq} as functions as functions of d_D from 0 nm to 200 nm. Three branches of N_{eq} were selected for the three ranges of d_D : (0 nm, 87 nm), (87 nm, 117 nm), and (117 nm, 200 nm). At $d_D = 113$ nm, equivalent extinction coefficient k_{eq} had a minimum value of 0.011 and equivalent index of refraction n_{eq} was 1.815. There were two ranges of d_D corresponding to low k_{eq} ($k_{eq} < 0.1$), which were from $d_D = 68$ nm to $d_D = 80$ nm and from $d_D = 99$ nm to $d_D = 115$ nm. With respect to real applications, the equivalent admittance $E = E_r + iE_i$ needed to be considered too. Figure 4b plots E_r and E_i as functions of d_D . High transmission required a small imaginary part of the admittance E_i . At $d_D = 108$ nm, E_i has a minimum magnitude of 0.091 and E_r was 4.078. The mismatch of the real part of the admittance between the cover medium and SFS can be improved through index-matching coatings to reduce reflection at the upper and bottom interfaces. For low-magnitude E_i ($|E_i| \leq 0.3$), E_r varied from 1.246 to 3.118 and 1.024 to 8.98 occurred during the ranges of ($d_D = 67$ nm, $d_D = 74$ nm) and ($d_D = 100$ nm, $d_D = 113$ nm), respectively. The ranges of d_D for low k_{eq} and low $|E_i|$ considerably

overlapped, thus a multilayer with low loss could be derived by tuning the dielectric layer within both ranges. The n_{eq} as a function of d_D and angle of incidence θ is shown in Figure 4c. The maximum n_{eq} is 2.156 at $\theta_0 = 90^\circ$ and $d_D = 126$ nm. At the range of d_D between 67 nm and 74 nm, the n_{eq} versus θ_0 showed that the SFS was equivalent to a dielectric-like anisotropic medium. The n_{eq} versus θ_0 showed near type I hyperbolic shape at the range from $d_D = 100$ nm to $d_D = 113$ nm. The optimum transmission for the metamaterial in air was considered here. The transmittance of Air/SFS/Air was greater than T_{min} from $\theta_0 = 0^\circ$ to $\theta_0 = 60^\circ$. The thickness d_D was tuned in the range that corresponded to type I hyperbolic metamaterial to yield a maximum T_{min} of 47.56% at $d_D = 100$ nm. Figure 4d plots the iso-frequency curve of Ag (20 nm)/Ta₂O₅ (100 nm)/Ag (20 nm)/Ta₂O₅ (100 nm)/Ag (20 nm), where k_0 was the wave vector in free space. Unlike a smooth and typical hyperbolic curve, the ratio k_z/k_0 kept around 1.2 within the range of k_x/k_0 between +1.56 and -1.56. It means that the reflected or diffracted ray vector was perpendicular to the interface for the parallel-to-interface component of the wave vector during the aforementioned range.

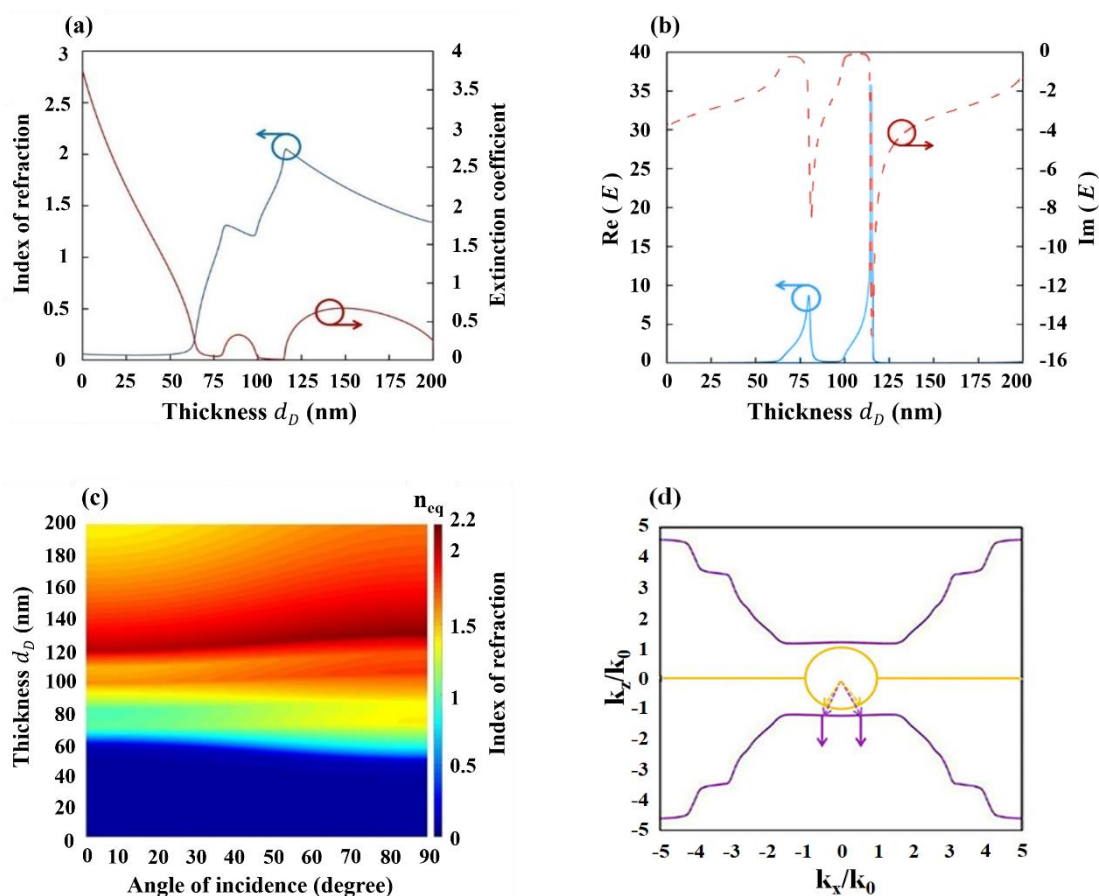


Figure 4. (a) n_{eq} and k_{eq} as functions of d_D of five-layered MDMDM at a wavelength of 600 nm, (b) E_r and E_i as functions of d_D of five-layered MDMDM a wavelength of 600 nm, (c) n_{eq} as a function of d_D and angle of incidence θ_0 at a wavelength of 600 nm, (d) the iso-frequency curve of Ag(20 nm)/Ta₂O₅ (100 nm)/Ag (20 nm)/ Ta₂O₅ (100 nm)/Ag (20 nm). The dotted arrows and solid arrows represent wave vector and ray vector, respectively.

The procedure for constructing the aforementioned modified FP SFS can be executed for a seven-layered MDMDMDM for a wavelength of 600 nm with 20 nm-thick Ag films and equally thick Ta₂O₅ films. Figure 5a shows n_{eq} and k_{eq} as functions of d_D . Figure 5b shows E_r and E_i as functions of d_D . There are three ranges of d_D corresponding to low k_{eq} ($k_{eq} < 0.1$), which were d_D : (64 nm, 67 nm), (83 nm, 97 nm), and (108 nm, 117 nm). The thickness of the dielectric layer in the seven-layered SFS with a low extinction coefficient was less than that of MDMDM. At $d_D = 113$ nm, E_i had a

minimum magnitude of 0.1327 and the E_r was 4.2736. E_r varied from 1.28 to 4.02 and 2.037 to 9.053 at a low-magnitude E_i ($|E_i| \leq 0.3$), which ranges were ($d_D = 84$ nm, $d_D = 92$ nm) and ($d_D = 110$ nm, $d_D = 116$ nm), respectively. The N_{eq} as a function of d_D and angle of incidence θ is shown in Figure 5c. The type I hyperbolic metamaterial occurred at d_D and ranged from 75 nm to 80 nm. The maximum T_{min} of 46.49 % occurred at $d_D = 85$ nm, and the corresponding iso-frequency curve is shown in Figure 5d. The optimum thickness for type I iso-frequency curve was shifted from $d_D = 100$ nm in MDMDM structure to $d_D = 80$ nm here in MDMDMDM structure. Compared with the five-layered case, the ratio k_z/k_0 keeps around 1.1 within a smaller range of k_x/k_0 between +1.7 and -1.7.

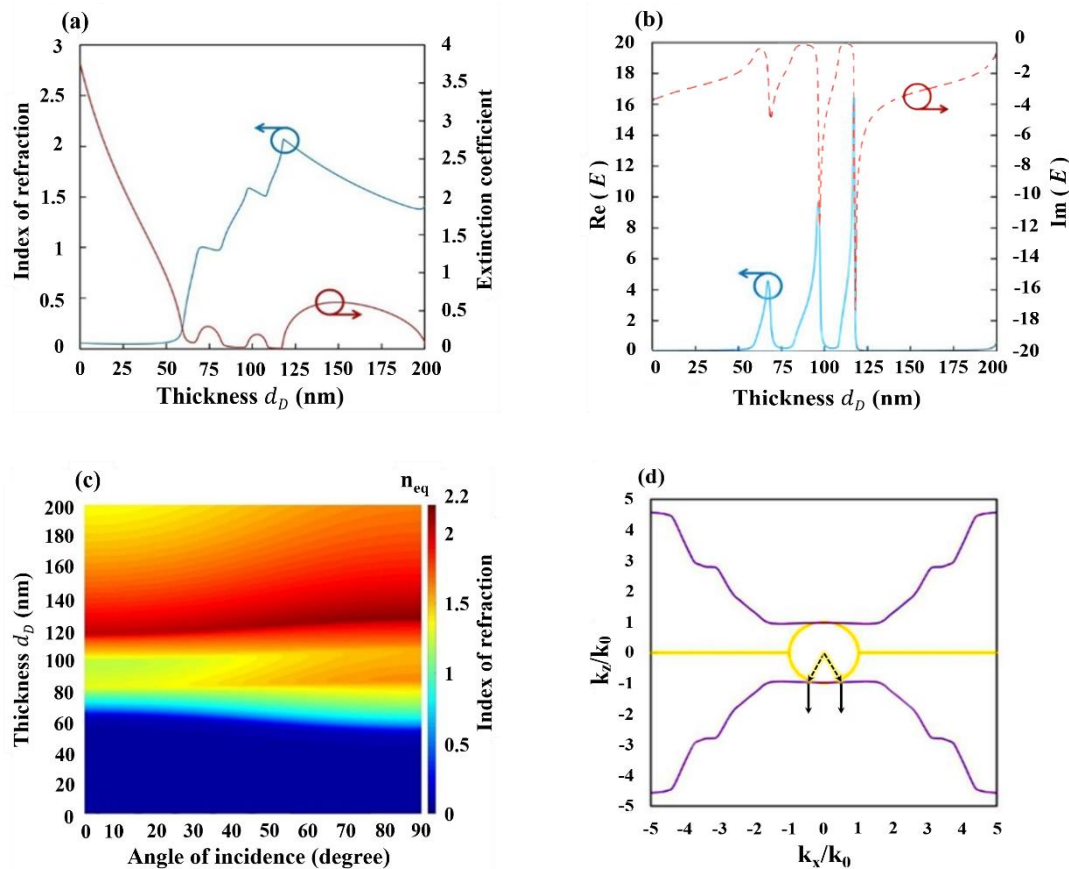


Figure 5. (a) n_{eq} and k_{eq} as functions of d_D of seven-layered MDMDM at a wavelength of 600 nm, (b) E_r and E_i as functions of d_D of seven-layered MDMDM a wavelength of 600 nm, (c) n_{eq} as a function of d_D and angle of incidence θ_0 at a wavelength of 600 nm, (d) the iso-frequency curve of Ag (20 nm)/Ta₂O₅ (85 nm)/Ag (20 nm)/ Ta₂O₅ (85 nm)/Ag (20 nm). The dotted arrows and solid arrows represent wave vector and ray vector, respectively.

4. Conclusions

In conclusion, the equivalent model of a symmetrical film stack was applied to calculate the precise equivalent refractive index and admittance. In order to satisfy the criteria of branch selection, the correct branch solution of the refractive index was only valid for a certain range of wavelength or thickness of the dielectric layer. We clarify that the previous stratiform metamaterial is a type I hyperbolic metamaterial instead of a negative index medium. Based on the modified Fabry-Perot design for a metal-dielectric multilayer, a low loss hyperbolic metamaterial can be designed for an odd-numbered metal-dielectric symmetrical film stack. It is demonstrated that the required thickness of dielectric film for a type I metamaterial can be reduced by increasing the number of films in a symmetrical film stack. A metal-dielectric multilayer should be arranged as a multiple symmetrical

film stack to exhibit the exact optical property. The method we proposed here can be applied to design a hyperbolic metamaterial in a precise and more flexible way.

Author Contributions: Y.-J.J. conceived the design method and supervised the data analysis. Y.-J.J. wrote the manuscript. W.-C.L. performed the calculations. W.-C.L. analyzed and checked all computational data.

Funding: Ministry of Science and Technology, Taiwan No. MOST 108-2221-E-027-100-MY3.

Acknowledgments: This work was supported by grants from the National Taipei University of Technology and the Ministry of Science and Technology, Taiwan.

Conflicts of Interest: The authors declare no conflicts of interest.

References

1. Pendry, J.B. Negative Refraction Makes a Perfect Lens. *Phys. Rev. Lett.* **2000**, *85*, 3966–3969. [[CrossRef](#)] [[PubMed](#)]
2. Shelby, R.A.; Smith, D.R.; Schultz, S. Experimental Verification of a Negative Index of Refraction. *Science* **2001**, *292*, 77–79. [[CrossRef](#)] [[PubMed](#)]
3. Liu, Y.; Zhang, X. Metamaterials: A new frontier of science and technology. *Chem. Soc. Rev.* **2011**, *40*, 2494–2507. [[CrossRef](#)] [[PubMed](#)]
4. Sun, J.; Litchinitser, N.M.; Zhou, J. Indefinite by Nature: From Ultraviolet to Terahertz. *ACS Photonics* **2014**, *1*, 293–303. [[CrossRef](#)]
5. Lu, L.; Simpson, R.E.; Valiyaveedu, S.K. Active hyperbolic metamaterials: Progress materials and design. *J. Opt.* **2018**, *20*, 103001. [[CrossRef](#)]
6. Verhagen, E.; de Waele, R.; Kuipers, L.; Polman, A. Three-dimensional negative index of refraction at optical frequencies by coupling plasmonic waveguides. *Phys. Rev. Lett.* **2010**, *105*, 223901. [[CrossRef](#)]
7. Xu, T.; Agrawal, A.; Abashin, M.; Chau, K.J.; Lezec, H.J. All-angle negative refraction and active flat lensing of ultraviolet light. *Nature* **2013**, *497*, 470–474. [[CrossRef](#)]
8. Yin, X.; Zhu, H.; Guo, H.; Deng, M.; Xu, T.; Gong, Z.; Li, X.; Hang, Z.H.; Wu, C.; Li, H.; et al. Hyperbolic Metamaterial Devices for Wavefront Manipulation. *Laser Photonics Rev.* **2019**, *13*, 1800081. [[CrossRef](#)]
9. Agranovich, V.M.; Kravtsov, V.E. Notes on crystal optics of superlattices. *Solid State Commun.* **1985**, *55*, 85–90. [[CrossRef](#)]
10. Hoffman, A.J.; Alekseyev, L.; Howard, S.S.; Franz, K.J.; Wasserman, D.; Podolskiy, V.A.; Narimanov, E.E.; Sivco, D.L.; Gmachl, C. Negative refraction in semiconductor metamaterials. *Nat. Mater.* **2007**, *6*, 946–950. [[CrossRef](#)]
11. Poddubny, A.; Iorsh, I.; Belov, P.; Kivshar, Y. Hyperbolic metamaterials. *Nat. Photonics* **2013**, *7*, 948–957. [[CrossRef](#)]
12. Maas, R.; Verhagen, E.; Parsons, J.; Polman, A. Negative refractive index and higher-order harmonics in layered metallodielectric optical metamaterials. *ACS Photonics* **2014**, *1*, 670–676. [[CrossRef](#)]
13. Macleod, H.A. *Thin-Film Optical Filters*, 4th ed.; CRC Press: Boca Raton, FL, USA, 2010; pp. 177–187.
14. Smith, D.R.; Vier, D.C.; Koschny, T.; Soukoulis, C.M. Electromagnetic parameter retrieval from inhomogeneous metamaterials. *Phys. Rev. E* **2005**, *71*, 036617. [[CrossRef](#)] [[PubMed](#)]
15. Kildishev, A.V.; Cai, W.; Chettiar, U.K.; Yuan, H.-K.; Sarychev, A.K.; Drachev, V.P.; Shalaev, V.M. Negative refractive index in optics of metal–dielectric composites. *J. Opt. Soc. Am. B* **2006**, *23*, 423–433. [[CrossRef](#)]
16. Jen, Y.-J.; Lin, M.-J.; Wu, H.-M.; Liao, H.-S.; Dai, J.-W. An interference coating of metamaterial as an ultrathin light absorber in the violet-to-infrared regime. *Opt. Express* **2013**, *21*, 10259–10268. [[CrossRef](#)] [[PubMed](#)]
17. Epstein, L.I. The design of optical filter. *J. Opt. Soc. Am.* **1952**, *42*, 806–810. [[CrossRef](#)]
18. Jen, Y.J.; Liu, W.C.; Chen, T.K.; Lin, S.W.; Jhang, Y.C. Design and deposition of a metal-like and admittance-matching metamaterial as an ultra-thin perfect absorber. *Sci. Rep.* **2017**, *7*, 3076. [[CrossRef](#)]
19. Jen, Y.J.; Lakhtakia, A.; Yu, C.W.; Jhou, J.J.; Wang, W.H.; Lin, M.J.; Wu, H.M.; Liao, H.S. Silver/silicon dioxide/silver sandwich films in the blue-to-red spectral regime with negative-real refractive index. *Appl. Phys. Lett.* **2011**, *99*, 181117. [[CrossRef](#)]
20. Chen, X.; Zhang, C.; Yang, F.; Liang, G.; Li, Q.; Guo, L.J. Plasmonic Lithography Utilizing Epsilon Near Zero Hyperbolic Metamaterial. *ACS Nano* **2017**, *11*, 9863–9868. [[CrossRef](#)]

21. Jen, Y.J.; Lee, C.C.; Lu, K.H.; Jheng, C.Y.; Chen, Y.J. Fabry-Perot based metal-dielectric multilayered filters and metamaterials. *Opt. Express* **2015**, *23*, 33008–33017. [[CrossRef](#)]
22. Zhu, P.; Shi, H.; Guo, L.J. SPPs Coupling Induced Interference in Metal/dielectric Multilayer Waveguides and Its Application for Plasmonic Lithography. *Opt. Express* **2012**, *20*, 12521–12529. [[CrossRef](#)] [[PubMed](#)]
23. Essential Macleod by Thin Film Center Inc. Available online: <http://www.thinfilmcenter.com> (accessed on 25 March 2013).



© 2019 by the authors. Licensee MDPI, Basel, Switzerland. This article is an open access article distributed under the terms and conditions of the Creative Commons Attribution (CC BY) license (<http://creativecommons.org/licenses/by/4.0/>).